Inorganic Chemistry
Article

Inorg. Chem. **2009**, *48*, 8115–8119 **8115**
DOI: 10.1021/ic900829z

Second-Order Nonlinear Optical Properties of Trisubstituted Keggin and Wells−Dawson Polyoxometalates: Density Functional Theory Investigation of the Inorganic Donor-Conjugated Bridge−Acceptor Structure

Chun-Guang Liu,[†,‡] Wei Guan,[†,‡] Ping Song,[†,‡] Zhong-Min Su,[*,†,‡] Chan Yao,[†,‡] and En-Bo Wang[*,‡]

[†]*Institute of Functional Material Chemistry and* [‡]*Key Laboratory of Polyoxometalate Science of Ministry of Education and Faculty of Chemistry, Northeast Normal University, Changchun 130024, P. R. China*

Received December 12, 2008

The donor-conjugated bridge−acceptor (D-A) model, as a simple molecular scheme, has been successfully used in the development of second-order organic compound, organometallic compound, and metal complex nonlinear optical (NLO) materials. However, for the totally inorganic molecules, the use of this model is still prohibitive. In the present paper, time-dependent density functional theory (TDDFT) was used to investigate the second-order NLO properties of vanadium- and molybdenum-trisubstituted Keggin and Wells−Dawson polyoxometalates (POMs). The results show that these POM clusters possess D-A structures. The oxygen atoms in the cap region and metal (vanadium and molybdenum) atoms in another cap region in these POM clusters can be viewed as the electron donor and acceptor, respectively. The vanadium ion derivatives possess larger second-order NLO responses and dipole moment than molybdenum ions derivatives; thus, the three vanadium atoms in the cap region act as a strong acceptor related to the three molybdenum atoms in cap region in our D-A scheme. The vanadomolybdate with Wells−Dawson structure displays the good second-order NLO response because of the relevant long conjugated bridge and strong acceptor. This D-A model may be an effective approach for optimizing the first hyperpolarizabilities of inorganic POM clusters.

1. Introduction

The totally inorganic nonlinear optical (NLO) materials have attracted considerable attention because of their good stability relative to organic compounds, organometallic compounds, and transition metal complexes. For about four decades, many kinds of inorganic NLO materials have been reported, such as inorganic salts,[1] inorganic oxides, semiconductors, and cluster compounds.[2] Among them, only some inorganic oxide NLO materials including KH_2PO_4 (KDP), $LiNbO_3$, β-BaB_2O_4 (BBO), and LiB_3O_5 (LBO) have been successfully commercialized.[3] Compared to organic NLO materials, the relevant small photoelectric coefficients of inorganic NLO materials are the bottleneck in practical applications.

Polyoxometalates (POMs) are early transition metal oxo clusters, this class of inorganic compounds is unmatched not only in terms of molecular structural diversity but also regarding reactivity and relevance to analytical chemistry, catalysis, medicine and materials science.[4] POMs reveal a huge variety of shapes, sizes, and compositions and provide a good basis for molecular design. Among them, Keggin and Wells-Dawson (W-D) POMs are the typical and important structures. The traditional Keggin and W-D POMs are centrosymmetric. However, a prerequisite to second-order NLO molecular materials is the molecular noncentrosymmetry. To achieve second-order NLO responses, POMs must be arranged noncentrosymmetrically; this has been achieved by means of (i) lacunary Keggin POMs structure, such as, a recent paper[5] reported that the nanocluster crystals of lacunary Keggin POMs Na_{10}-$XW_9O_{34}\cdot 18H_2O$ (X = Si, Ge) and $K_7PW_9Mo_2O_{39}\cdot 18H_2O$ had higher NLO responses than KDP by the powder second-harmonic-generation (SHG) measurement; (ii) an efficient noncentrosymmetric arrangement of POM crystal by introducing some special counterions, the measurement[6]

*To whom correspondence should be addressed. E-mail addresses: zmsu@nenu.edu.cn (Z.-M.S.); wangenbo@public.cc.jl.cn (E.-B.W.).

(1) (a) Wes, R. S.; Gaylord, T. K. *Appl. Phys. A: Mater. Sci. Process.* **1985**, *37*, 191. (b) Klein, M. B.; Dunning, G. J.; Valley, G. C.; Lind, R. C.; O'Meara, T. R. *Opt. Lett.* **1986**, *11*, 575.

(2) (a) Hou, H. W.; Wei, Y. L.; Song, Y. L.; Mi, L. W.; Tang, M. S.; Li, L. K.; Fan, Y. T. *Angew. Chem., Int. Ed.* **2005**, *44*, 6067. (b) Chen, X. H.; Wu, K. C.; Snijders, J. G.; Lin, C. S. *Inorg. Chem.* **2003**, *42*, 532. (c) Nie, W. *Adv. Mater.* **1993**, *5*, 520.

(3) (a) Smith, W. L. O. *Appl. Opt.* **1977**, *16*, 798. (b) Boyd, G. D.; Miller, R. C.; Nassau, K.; Bond, W. L.; Savage, A. *Appl. Phys. Lett.* **1964**, *16*, 1856. (c) Chen, C.; Wu., B.; Jiang, A.; You, G. *Sci. Sin. Ser. B* **1985**, 235. (d) Chen, C.; Wu, Y.; Jiang, A.; Wu, B.; You, G.; Li, R.; Lin, S. *J. Opt. Soc. Am.* **1989**, *B6*, 616.

(4) Hill, C. L. *Chem. Rev.* **1998**, *98*, 1.

(5) Murakami, H.; Kozeki, T.; Suzuki, Y.; Ono, S.; Ohtake, H.; Sarukura, N. *Appl. Phys. Lett.* **2001**, *79*, 3564.

(6) Xie, Y.-M.; Zhang, Q.-S.; Zhao, Z.-G.; Wu, X.-Y.; Chen, S.-C.; Lu, C.-Z. *Inorg. Chem.* **2008**, *47*, 8086.

Published on Web 07/29/2009

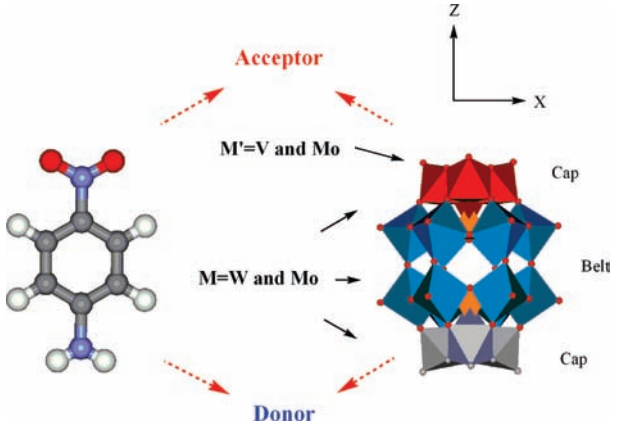

Figure 1. Polyhedral representation of the donor−acceptor substituted Wells-Dawson structure. The gray and red octahedrons can be viewed as the electron donor and acceptor in this scheme, respectively. By contrast, a *p*-nitroaniline molecule is listed here.

of powder SHG effect of $[H_3O](C_{12}H_{10}N_3)_2$ $(PW_{12}O_{40})$ showed that it exhibited a SHG efficiency of about 2 times than that of KDP (Keggin POM anion in this crystal, $[PW_{12}O_{40}]^{3-}$, has centrosymmetry). All of the results showed that POMs possessed considerably large second-order NLO responses in inorganic NLO materials. Nevertheless, the two reported methods are not effective for optimizing their second-order NLO responses.

The donor-conjugated bridge-acceptor (D-A) dipole structure, as a simple molecular scheme, has been successfully used in the development of second-order organic NLO materials. However, the usage of this scheme was just limited in organic, organometallic, and metal complex molecules.[7] By contrast, inorganic molecules are hard to be modified to obtain the D−A structures (besides the organic−inorganic hybrids).[8] In the past two decades, the locations of added electrons in transition metal trisubstituted Keggin and W-D POM clusters have been determined by using ^{183}W and ^{31}P nuclear magnetic resonance (NMR) and X-band electron spin resonance (ESR) spectroscopic measurements.[9] These results showed that the added electrons localized on the three substituted transition metal atoms of these POM clusters. Density functional theory (DFT) calculations showed that the LUMO of these trisubstituted Keggin and W-D POMs are mainly localized on the three substituted transition metal atoms.[10] All of these results indicated that transition metal trisubstituted effect of Keggin and W-D POMs leads to the charge separation, the metal atoms in cap region may be viewed as the electron acceptor (see Figure 1).

In this work, we employ time-dependent density functional theory (TDDFT) method to calculate the second-order NLO properties of typical transition metal trisubstituted Keggin and W-D clusters α-$[PM_9M'_3O_{40}]^{n-}$ and α-$[P_2M_{15}M'_3O_{62}]^{m-}$, M = W(VI), Mo(VI), and M′ = V(V), Mo(VI), to verify the relationship between second-order NLO properties and D-A structures. We hope that our present work can provide qualitative information for optimizing the second-order NLO properties of these inorganic NLO clusters. According to the literature,[10] the geometrical optimizations of all clusters are under C_{3v} symmetry constraint, and the shorthand notation without oxygen atoms and charge has been used in this paper.

2. Computational Details

All optimization were carried out using the BP86[11] generalized gradient approximations and VWN[12] local density functional, triple-ζ basis plus polarization Slater-type orbital basis sets (TZP),[13] and the integration parameter 6.0, as implemented in the ADF 2006 program system.[13] It is well-known that the NLO properties of atoms are closely associated with the valent electrons, thus, the innermost atomic shells are kept frozen for speeding up the computation. The frozen core orbitals, which are solutions of a large-basis all-electron calculation on the isolated atom, are expressed in an auxiliary set of (Slater-type) basis functions in ADF program.[14] The internal or core electrons (O, 1s; P, V, 1s-2p; Mo, 1s-3d; W, 1s-4d) were described by single Slater functions in this work. The relativistic effects were taken into account by using the zero-order regular approximation (ZORA).[15] For the large molecules, high-level quantum chemical calculations are very computationally demanding. Thanks much to the work of Poblet and co-worker, we employed ADF 2006 program to optimize these clusters based on the equilibrium structures provided by Poblet in ref 10.

In the present paper, TDDFT calculation was adopted to obtain the molecular hyperpolarizability and electronic structure. To the best of our knowledge, adequate approximation of the Kohn−Sham exchange-correlation (XC) potential ν_{xc} remains a challenging problem because the exact form of ν_{xc} is not known. Thus, various approximations are in use. The traditional local density approximations and generalized gradient approximations for ν_{xc} do not have the correct asymptotic behavior for large interelectron distances and excitation energies. To overcome this problem, Van Leeuwen−Baerends (LB94) potential[16] has been developed for satisfying the correct asymptotic conditions. However, the improvements of this potential do not hold for all properties, several papers have pointed out that DFT based on current conventional XC functionals overestimated the first hyperpolarizability of D-A systems because of the excessive charge transfer (CT) between donor and acceptor.[17] In this work, the asymptotically correct LB94 potential has been adopted to calculate the electronic structures and hyperpolarizabilities of all clusters. As a check on the asymptotic correction in LB94 functional for hyperpolarizability, the BP86 functional and hybrid functional, PBE0,[18] containing 25% Hartree−Fock

(7) Kanis, D. R.; Ratner, M. A.; Marks, T. J. *Chem. Rev.* **1994**, *94*, 195.
(8) (a) Datta, A.; Mallajosyula, S. S.; Pati, S. K. *Acc. Chem. Res.* **2007**, *40*, 213. (b) Innocenzi, P.; Lebeau, B. *J. Mater. Chem.* **2005**, *15*, 3821. (c) Datta, A. D.; Pati, S. K. *J. Phys. Chem. A.* **2004**, *108*, 9527.
(9) (a) Kozik, M.; Hammer, C. F.; Bader, L. C. W. *J. Am. Chem. Soc.* **1986**, *108*, 2748. (b) Kozik, M.; Hammer, C. F.; Bader, L. C. *J. Am. Chem. Soc.* **1986**, *108*, 7627. (c) Harmalder, S. P.; Pope, M. T. *J. Am. Chem. Soc.* **1981**, *103*, 7381.
(10) Lopez, X.; Bo, C.; Poblet, J. M. *J. Am. Chem. Soc.* **2002**, *124*, 12574.
(11) (a) Becke, A. D. *Phys. Rev. A* **1988**, *38*, 3098. (b) Perdew, J. P. *Phys. Rev. B* **1986**, *33*, 8822.
(12) Vosko, S. H.; Wilk, L.; Nusair, M. *Can. J. Phys.* **1980**, *58*, 1200.
(13) (a) Te Velde, G.; Bickelhaupt, F. M.; Baerends, E. J.; Fonseca Guerra, C.; van Gisbergen, S. J. A.; Snijders, J. G.; Ziegler, T. *J. Comput. Chem.* **2001**, *22*, 931. (b) Fonseca Guerra, C.; Snijders, J. G.; Te Velde, G.; Baerends, E. J. *Theor. Chem. Acc.* **1998**, *99*, 391. (c) *ADF2006.01*; SCM, Theoretical Chemistry,Vrije Universiteit, Amsterdam, The Netherlands, **2006**; http://www.scm.com.
(14) Schreckenbach, G.; Ziegler, T. *Int. J. Quantum Chem.* **1996**, *60*, 753 and references therein.
(15) (a) Chang, C.; Pelissier, M.; Durand, M. *Phys. Scr.* **1986**, *34*, 394. (b) van Lenthe, E.; Baerends, E. J.; Snijders, J. G. *J. Chem. Phys.* **1993**, *99*, 4597. (c) van Lenthe, E.; Baerends, E. J.; Snijders, J. G. *J. Chem. Phys.* **1994**, *101*, 9783.
(16) van Leeuwen, R.; Baerends, E. J. *Phys. Rev. A* **1994**, *49*, 2421.
(17) Bulat, F. A.; Toro-Labbe, A.; Champagne, B.; Kirtman, B.; Yang, W. *J. Chem. Phys.* **2005**, *123*, 14319 and references therein.
(18) (a) Grimme, S. *J. Comput. Chem.* **2004**, *25*, 1463. (b) Ernzerhof, M.; Scuseria, G. *J. Chem. Phys.* **1999**, *110*, 5029.

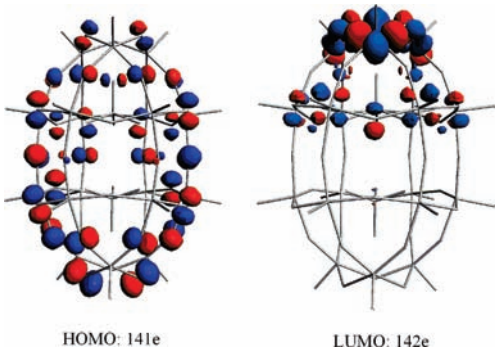

Figure 2. Frontier molecular orbitals of $P_2W_{15}V_3$ obtained by LB94/TZP calculation.

(HF) exchange were also used for all hyperpolarizability calculations.

The linear and nonlinear polarizabilities (hyperpolarizabilities) can be defined through an expansion of the dipole moment (μ) into different order of the external fields (E)

$$\mu_a = \mu_a(E^b = E^c = E^d \quad \ldots = 0) + \sum_b \alpha_{ab}E^b + \frac{1}{2!}\sum_{bc}\beta_{abc}E^bE^c + \frac{1}{3!}\sum_{bcd}\gamma_{abcd}E^bE^cE^d + \quad \ldots \qquad (1)$$

where α is the linear polarizability tensor, β and γ are the second- and third-order polarizability tensor, respectively. And a, b, and c label the x, y, and z components. In ADF program, the linear response equation of TDDFT[19] is adopted to compute linear polarizability, α, the $(2n + 1)$-theorem[20] is used for obtaining β. TDDFT method has been broadly applied to investigate the NLO responses of organic, inorganic compounds and nanosized species.[21]

3. Results and Discussion

3.1. Donor−Acceptor Model for These Clusters. Although the details of the electronic structure of trisubstituted Keggin and W-D clusters have been studied before,[10] we review some important results here since these will be necessary for our analysis of the D-A model in the next section. The trisubstituted Keggin and W-D clusters present the typical molecular orbitals distributions of POMs, where the occupied oxo ligand orbitals and the empty set of d-like metal orbitals are separated. Figure 2 shows the relevant frontier orbitals of W-D cluster $P_2W_{15}V_3$. It can be found that the HOMO of $P_2W_{15}V_3$ is delocalized over the oxygen atoms of cage surface. The LUMO is mainly localized on the vanadium atoms in cap region. As is clearly seen from Figure 2, an excitation corresponding to the HOMO → LUMO orbital transition would give the CT from the oxygen atoms of cage to the vanadium atoms. Hence, our analysis supports that this cluster possesses D-A structure. A more complete characterization of the electronic excitations in all clusters based on the TDDFT calculations will be given in the next section.

3.2. Spectrum Properties of All Clusters. We have performed TDDFT calculations to obtain electronic spectrum. It should be stressed that the TDDFT method sometimes underestimates the excitations energies involving CT excited states because of the incorrect long-range behaviors of the exchange potential compared to the multireference configuration interaction (MRCI) method, but it is the most accurate method that can be used on large molecules at an affordable computational cost. The TDDFT calculated transition energies, oscillator strength of first excited state and crucial excited state, together with orbital transition of the most important contributions to these excited states are summarized in Table 1. The crucial excited stat is the lowest excited state with substantial oscillator strength according to the TDDFT calculations. We take cluster $P_2Mo_{15}V_3$ for an example to analyze the electronic transition. The first excited state of $P_2Mo_{15}V_3$ is generated by the promotion of one electron from HOMO to LUMO. Due to the little overlap between the two orbitals, such electronic transitions are forbidden, reflecting the small oscillator strength (f_{os}) (see Figure 2 and Table 1). However, the orbital transitions associated with the crucial excited states are allowed according to the transition selection rules, and thus the calculated oscillator strength of crucial excited state is larger than that of first excited states. The orbital transitions associated with the crucial excited state of $P_2Mo_{15}V_3$ are shown in Figure 3, it can be seen that the excitation contains 39a2 → 41a2 and 99e → 107e transitions. The two occupied orbitals (39a2 and 99e) are mainly localized on oxygen atom in cap region, and the two unoccupied orbitals (41a2 and 107e) are localized on the V atoms and adjacent W atoms (see Figure 3). These excitations mostly consist of CT from oxo ligands of cap region to V atoms and adjacent W atoms. The results show that the oxygen atoms of cap region display the electron donor features, and the V atoms in another cap region display electron acceptor properties.

3.3. Second-Order NLO Properties for Donor−Acceptor Model. The static hyperpolarizabilities, β_{vec}, for all clusters, have been calculated by using the following equation:

$$\beta_i = \beta_{iii} + \frac{1}{3}\sum_{i\neq j}(\beta_{ijj} + \beta_{jij} + \beta_{jji}) \qquad (2)$$

Using the x, y, z components, the magnitude of the hyperpolarizability tensors can be calculated by

$$\beta_{vec} = \sum_i \mu_i\beta_i/|\mu| \quad i = x,y,z \qquad (3)$$

All the clusters belong to C_{3v} symmetry group; for a molecule of C_{3v} symmetry, there are only five nonzero individual β tensor components, β_{xxz}, β_{xzx}, β_{zxx}, β_{zzz}, and β_{yyy}. In addition, the CT direction of all POM clusters lies in the Z axis (see Figure 1); thus, the β_{zzz} and

(19) Gross, E. K. U. ; Kobson, J. F.; Petersilka, M. In *Density Functional Theory*; Nalewajski, R. F., Ed.; Topics in Current Chemistry; Springer: Heidelberg, Germany, 1996.

(20) van Gisbergen, S. J. A.; Snijders, J. G.; Baerends, E. J. *J. Chem. Phys.* **1998**, *109*, 10644; Erratum 1999, 111, 6652.

(21) (a) van Gisbergen, S. J. A.; Snijder, J. G.; Baerends, E. J. *Phys. Rev. Lett.* **1997**, *78*, 3097. (b) van Gisbergen, S. J. A.; Snijder, J. G.; Baerends, E. J. *J. Chem. Phys.* **1998**, *109*, 10657. (c) Hieringer, W.; Evert, J. B. *J. Phys. Chem. A* **2006**, *110*, 1014. (d) Powell, C. E.; Cifuenties, M. P.; Morrall, J. P.; Stranger, R.; Humphrey, M.; G.; Samoc, M.; Luther-Davies, B.; Heath, G. A. *J. Am. Chem. Soc.* **2003**, *125*, 602.

Table 1. LB94/TZP Calculated Excited State Transition Energy (ΔE_{ge}, eV), Oscillator Strengths (f_{os}), and Major Assignment of Optical Transitions for All Clusters

clusters	excited state (symmetry)	ΔE_{ge}	f_{os}	composition	major assignment
			Keggin clusters		
PW_9V_3	S1(E)	1.878	0.000	90e → 91e (92.3%)	oxo ligand → V cap
	S6(A1)	2.476	0.004	88e → 91e (53.5%)	oxo ligand → V cap
				89e → 91e (23.5%)	oxo ligand → V cap
PMo_9V_3	S1(A1)	1.742	0.000	69e → 70e (95.7%)	oxo ligand → V cap
	S5(E)	2.041	0.002	24a2 → 70e (32.4%)	oxo ligand → V cap
				67e → 70e (42.3%)	oxo ligand → V cap
PW_9Mo_3	S1(E)	2.204	0.000	90e → 91e (93.2%)	oxo ligand → Mo cap
	S32(A1)	3.483	0.020	90e → 94e (20.8%)	oxo ligand→W belt
				55a1 → 57a1 (10.4%)	oxo ligand → Mo cap
				82e → 92e (17.0%)	oxo ligand → W belt
				88e → 93e (12.5%)	oxo ligand→Mo cap
			Wells−Dawson clusters		
$P_2W_{15}V_3$	S1(E)	1.714	0.000	141e → 142e (100%)	oxo ligand → V cap
	S31(A1)	2.721	0.032	55a2 → 58a2 (29.1%)	oxo ligand → W belt
				56a2 → 58a2 (27.6%)	oxo ligand → W belt
				56a2 → 59a2 (15.2%)	oxo ligand → V cap
$P_2Mo_{15}V_3$	S1(E)	1.061	0.000	106e → 107e (100%)	oxo ligand → V cap
	S14(A1)	1.986	0.015	39a2 → 41a2 (49.4%)	oxo ligand → Mo belt
				99e → 107e (28.9%)	oxo ligand → V cap + Mo
$P_2W_{15}Mo_3$	S1(E)	1.823	0.000	141e → 58a2 (100%)	oxo ligand → W belt
	S15(A1)	2.558	0.042	55a2 → 58a2 (18.7%)	oxo ligand → W belt
				135e → 142e (27.9)	oxo ligand → Mo cap + W
				134e → 142e (14.6%)	oxo ligand → Mo cap + W

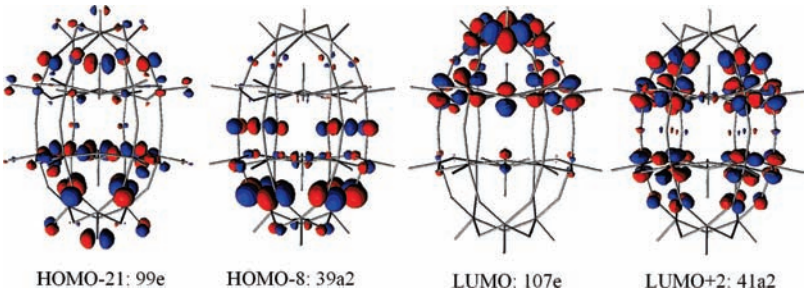

Figure 3. Molecular orbitals of $P_2Mo_{15}V_3$ obtained by LB94/TZP calculation.

β_{zxx} components are larger than the other nonzero individual β tensor components. The β_{vec} values calculated by different functionals in ADF program have been listed in Table 2. It can be found that the β_{vec} values of all clusters are functional-dependent: (i) the BP86 results are very close to the PBE0 values, and thus 25% HF exchange in PBE0 functional is not important for our studied systems; (ii) the LB94 potential corrected by asymptotic behavior seems to overestimate the hyperpolarizabilities of vanadium ion derivatives and underestimate that of molybdenum ion derivatives in Keggin and W-D structures compared with the BP86 and PEB0 (see Table 2); (iii) the size effect of molecule does not significantly affect the differences among three functionals for β_{vec} values, such as, the LB94 value for relevant small system PW_9V_3, is ~1.18 times as large as BP86 and PEB0 results, as increase of cluster size, this value only increases to ~1.20 times in $P_2W_{15}V_3$. All the functionals yield the same order of β_{vec} values, $PW_9V_3 > PMo_9V_3 > PW_9Mo_3$ for Keggin clusters, and $P_2Mo_{15}V_3 > P_2W_{15}V_3 > P_2W_{15}Mo_3$ for W-D clusters.

As shown in Table 2, these clusters possess considerably large second-order NLO responses. W-D cluster

Table 2. Static Second-Order NLO Polarizabilities ($\times 10^{-30}$ esu) and Ground-State Dipole Moments (Debye) of All Clusters and *p*-Nitroaniline (PNA) Molecule Obtained by the LB94, BP86, and PBE0 Functionals with TZP Basis Sets

clusters	functionals	β_{zzz}	β_{zxx}	β_{vec}	$\lvert\mu_G\rvert$
PW_9V_3	LB94	−5.979	−4.430	−8.904	1.209
	BP86	−4.662	−3.964	−7.554	1.033
	PBE0	−4.632	−4.014	−7.596	1.091
PMo_9V_3	LB94	−4.529	−3.226	−6.589	1.342
	BP86	−1.341	−2.421	−3.710	1.288
	PBE0	−0.652	−2.331	−3.188	1.355
PW_9Mo_3	LB94	−0.598	−1.505	−1.448	0.577
	BP86	−0.031	−1.737	−2.065	0.743
	PBE0	−0.029	−1.805	−2.183	0.767
$P_2W_{15}V_3$	LB94	−47.829	−5.398	−35.175	5.601
	BP86	−39.746	−4.558	−29.317	4.706
	PBE0	−40.267	−4.645	−29.734	4.785
$P_2Mo_{15}V_3$	LB94	−63.642	−5.085	−44.287	7.797
	BP86	−50.010	−3.186	−33.829	7.444
	PBE0	−48.553	−2.802	−32.494	7.597
$P_2W_{15}Mo_3$	LB94	−4.885	−1.153	−4.313	0.785
	BP86	−6.323	−1.451	−5.536	0.917
	PBE0	−6.797	−1.565	−5.956	0.926
PNA	LB94	−17.656	1.386	9.523	-
	BP86	−16.359	1.345	8.735	-
	PBE0	−16.310	1.390	8.668	-

$P_2Mo_{15}V_3$ displays the largest β_{vec} values among them, -44.287×10^{-30}esu, which is 11 times as large as that of $P_2W_{15}Mo_3$ according to the LB94 calculations. For a purpose of comparison, the static hyperpolarizability of *p*-nitroaniline (PNA) molecule has been calculated at the same theoretical level (LB94/BP86/PBE0/TZP) in ADF program (see Table 2). It can be found that the calculated static hyperpolarizability value of $P_2Mo_{15}V_3$ is about 5 times as large as that of organic PNA molecule according to our DFT calculations (see Table 2). As mentioned above, the SHG intensity of lacunary Keggin cluster crystal, $Na_{10}SiW_9O_{34}\cdot 18H_2O$, was 10.2 times as large as that of KDP according to the powder SHG measurement.[5] We have calculated the static hyperpolarizability of $[SiW_9O_{34}]^{10-}$ at LB94/TZP level in ADF program,[22] the results showed that β_{vec} value of this cluster was 11.13×10^{-30}esu, which is ~4 times smaller than $P_2Mo_{15}V_3$. All of the results indicate that the studied cluster has excellent second-order NLO properties in totally inorganic compounds.

The question we are now concerned with is the transition metal substituted effects in cap region, that is, the acceptor moiety in our D-A model (see Figure 1). For Keggin clusters, the three vanadium ions derivatives (PW_9V_3, PMo_9V_3) generate larger second-order NLO responses than that of three molybdenum ions derivative (PW_9Mo_3) (see Table 2). The β_{vec} value of PW_9V_3 is 6 times as large as that of PW_9Mo_3 according to LB94 results. This indicates that three vanadium atoms can be viewed as a stronger acceptor compared with the three molybdenum atoms in Keggin structure. However, the β_{vec} values of Keggin clusters are not sensitive to the substitution of the belt metal M (M = W(VI), Mo(VI)) compared with the replacement of cap metal M′ (M′ = V(V), Mo(VI)) (PW_9V_3 vs PMo_9V_3). To verify the acceptor features of vanadium and molybdenum atoms, we have calculated the second-order NLO properties of the same element W-D clusters with regard to the Keggin clusters. The β_{vec} values of W-D clusters are also listed in Table 2. As mentioned above, the three vanadium ions derivatives in W-D clusters also display larger second-order NLO responses than the three molybdenum ions derivative ($P_2W_{15}V_3$ and $P_2Mo_{15}V_3$ vs $P_2W_{15}Mo_3$). Thus, the three vanadium atoms are still a strong acceptor in W-D structure. Moreover, we noticed that belt metal substitutions also affect the second-order NLO responses in W-D structures ($P_2W_{15}V_3$ vs $P_2Mo_{15}V_3$). The second-order properties of $P_2Mo_{15}V_3$ are larger than that of $P_2W_{15}V_3$ according to our DFT calculations.

We try to explain the fact above by using D-A model. There are 12 equatorial metals (belt metal) in large sized W-D cluster. In our D-A scheme, the 12 equatorial metal atoms array can be viewed as the increase of the conjugated bridge length compared to Keggin cluster. The belt metal substitution is equal to tuning conjugated bridge; thus, the second-order NLO properties of W-D clusters are sensitive to the belt metal substitution and are larger than that of Keggin clusters because of the longer and tunable conjugated bridge

It is well-known that the dipole moment values of D−A molecules are determined by the donor and acceptor strength and the conjugated bridge. According to the above-mentioned discussions, the acceptor strength of three vanadium ions derivatives are larger than that of three molybdenum ions derivative; thus the dipole moments of vanadium ion derivatives should be larger than that of molybdenum ion derivatives in the same structure. Our DFT calculations well reproduce this trend, the dipole moments of three vanadium ions derivatives are larger than that of three molybdenum ions derivatives according to various functionals calculations (see Table 2). The computed dipole moment of $P_2Mo_{15}V_3$ is about 10 times as large as that of $P_2W_{15}Mo_3$. Thus, the ground-state molecules of three vanadium ions derivate clusters have higher degree of polarization.[23] Substitution effect of the conjugated bridge also affects the dipole moments of these clusters; for example, $P_2Mo_{15}V_3$ displays the larger ground-state dipole moment than that of $P_2W_{15}V_3$.

4. Conclusions

We have demonstrated that the vanadium and molybdenum trisubstituted Keggin and Wells-Dawson POM clusters possess donor-conjugated bridge-acceptor structures by using different functionals. The oxo ligands in cap region and vanadium/molybdenum atoms in another cap region can be viewed as the electron donor and acceptor, respectively. The three vanadium atoms in cap region is a strong acceptor compared with the three molybdenum atoms in our D-A scheme. The relevant long conjugated bridge and strong acceptor significantly enhance the second-order NLO response. The vanadomolybdate with Wells-Dawson structure displays good second-order NLO properties.

Acknowledgment. The authors gratefully acknowledge the financial support from the National Natural Science Foundation of China (Project No. 20573016), Chang Jiang Scholars Program (2006), Program for Changjiang Scholars and Innovative Research Team in University (IRT0714), Department of Science and Technology of Jilin Province (20082103), the Training Fund of NENU's Scientific Innovation Project (NENU-STC07017, -STC08005 and -STC08012), and Science Foundation for Young Teachers of Northeast Normal University (20090401). We also thank Yuhe Kan for computational support.

(22) Guan, W.; Yang, G. C.; Yan, L. K.; Su, Z. M. *Eur. J. Inorg. Chem.* **2006**, 4179.

(23) (a) Geskin, V. M.; Lambert, C.; Bredas, J. L. *J. Am. Chem. Soc.* **2003**, *125*, 15651. (b) Liu, C. G.; Qiu, Y. Q.; Su, Z. M.; Yang, G. C.; Sun, S. L. *J. Phys. Chem. C* **2008**, *112*, 7021.